Exploring the limits of single emitter detection in fluorescence and extinction

G. Wrigge[1], J. Hwang[1], I. Gerhardt[1,2], G. Zumofen[1], and V. Sandoghdar[1]

[1]*Laboratory of Physical Chemistry and opt ETH, ETH Zürich, CH-8093 Zürich, Switzerland*

[2]*Current address: CQT, Centre for Quantum Technologies, 3 Science Drive 2, 117543 Singapore*

vahid.sandoghdar@ethz.ch

Abstract: We present an experimental comparison and a theoretical analysis of the signal-to-noise ratios in fluorescence and extinction spectroscopy of a single emitter. We show that because of its homodyne nature the extinction measurements can be advantageous if the emitter is weakly excited. Furthermore, we discuss the potential of this method for the detection and spectroscopy of weakly emitting systems such as rare earth ions.

OCIS codes: (300.6390) Spectroscopy, molecular; (300.1030) Absorption; (270.1670) Coherent optical effects; (270.5585) Quantum information and processing.

References and links

1. F. Kulzer and M. Orrit, Single-Molecule Optics, Annu. Rev. Phys. Chem. **55**, 585–611 (2004).
2. W. E. Moerner and L. Kador, "Optical Detection and Spectroscopy of Single Molecules in a Solid," Phys. Rev. Lett. **62**, 2535–2538 (1989).
3. M. Orrit and J. Bernard, "Single Pentacene Molecules Detected by Fluorescence Excitation in a *p*-Terphenyl Crystal," Phys. Rev. Lett. **65**, 2716–2719 (1990).
4. E. Shera, N. Seitzinger, L. Davis, R. Keller, and S. Soper, "Detection of single fluorescent molecules," Chem. Phys. Lett. **174**, 553–557 (1990).
5. E. Betzig and R. J. Chichester, "Single Molecules Observed by Near-Field Scanning Optical Microscopy," Science **262**, 1422–1425 (1993).
6. S. Nie, D. T. Chiu, and R. N. Zare, "Probing Individual Molecules with Confocal Fluorescence Microscopy," Science **266**, 1018–1021 (1994).
7. T. Basche, W. E. Moerner, M. Orrit, and U. Wild, *Single Molecule Spectroscopy* (John Wiley and Sons, 1999).
8. T. Plakhotnik and V. Palm, "Interferometric signatures of single molecules," Phys. Rev. Lett. **87**, 183602 (2001).
9. J. R. Guest, T. H. Stievater, X. Li, J. Cheng, D. G. Steel, D. Gammon, D. S. Katzer, D. Park, C. Ell, A. Thränhardt, G. Khitrova, and H. M. Gibbs, "Measurement of optical absorption by a single quantum dot exciton," Phys. Rev. B. **65**, 241310(R) (2002).
10. B. Alen, F. Bickel, K. Karrai, R. J. Warburton, and P. M. Petroff, "Stark-shift modulation absorption spectroscopy of single quantum dots," Appl. Phys. Lett. **83**, 2235–2237 (2003).
11. I. Gerhardt, G. Wrigge, P. Bushev, G. Zumofen, M. Agio, R. Pfab, and V. Sandoghdar, "Strong extinction of a laser beam by a single molecule," Phys. Rev. Lett. **98**, 033601 (2007).
12. I. Gerhardt, G. Wrigge, M. Agio, P. Bushev, G. Zumofen, and V. Sandoghdar, "Scanning Near-Field Optical Coherent Spectroscopy of Single Molecules at 1.4 Kelvin," Opt. Lett. **32**, 1420–1422 (2007).
13. G. Wrigge, I. Gerhardt, J. Hwang, G. Zumofen, and V. Sandoghdar, "Efficient coupling of photons to a single molecule and the observation of its resonance fluorescence," Nature Phys. **4**, 60–66 (2008).
14. C. Cohen-Tannoudji, J. Dupont-Roc, and G. Grynberg, *Atom-Photon Interactions* (John Wiley & Sons, Inc., 1992).
15. D. Jackson, *Classical Electrodynamics* (Wiley and Sons, 1999).
16. H. A. Haus, *Electromagnetic Noise and Quantum Optical Measurements* (Springer-Verlag, Heidelberg, 2000).
17. H. P. Yuen and V. W. S. Chan, "Noise in homodyne and heterodyne detection," Opt. Lett. **8**, 177 (1983).

#98684 - $15.00 USD Received 11 Jul 2008; revised 18 Sep 2008; accepted 27 Sep 2008; published 14 Oct 2008

18. G. Zumofen, N. M. Mojarad, V. Sandoghdar, and M. Agio, "Perfect Reflection of Light by an Oscillating Dipole," Phys. Rev. Lett. (to appear), http://arxiv.org/abs/0805.3231v2 (2008).
19. W. E. Moerner, "Examining Nanoenvironments in Solids on the Scale of a Single, Isolated Impurity Molecule," Science **265**, 46–53 (1994).
20. T. Plakhotnik, "Absorption and coherent emission of single molecules," J. Lumin. **98**, 57–62 (2002).
21. A. N. Vamivakas, M. Atatüre, J. Dreiser, S. T. Yilmaz, A. Badolato, A. K. Swan, B. B. Goldberg, A. Imamoglu, and M. S. Ünlü, "Strong extinction of a far-field laser beam by a single quantum dot," Nano Lett. **7**, 2892–2896 (2007).
22. P. Kukura, M. Celebrano, A. Renn, and V. Sandoghdar, "Seeing a single quantum emitter in its bright and dark states," Nano Lett. (DOI: 10.1021/nl801735y), http://arxiv.org/abs/0802.1206 (2008).
23. A. A. Mikhailovsky, M. A. Petruska, M. I. Stockman, and V. I. Klimov, "Broadband near-field interference spectroscopy of metal nanoparticles using a femtosecond white-light continuum," Opt. Lett. **28**, 1686–1688 (2003).
24. K. Lindfors, T. Kalkbrenner, P. Stoller, and V. Sandoghdar, "Detection and spectroscopy of gold nanoparticle using supercontinuum white light confocal microscopy," Phys. Rev. Lett. **93**, 037401 (2004).
25. A. Arbouet, D. Christofilos, N. D. Fatti, F. Vallée, J. R. Huntzinger, L. Arnaud, P. Billaud, and M. Broyer, "Direct measurement of the single-metal-cluster optical absorption," Phys. Rev. Lett. **93**, 127401 (2004).
26. V. Jacobsen, P. Stoller, C. Brunner, V. Vogel, and V. Sandoghdar, "Interferometric optical detection and tracking of very small gold nanoparticles at a water-glass interface," Opt. Express **14**, 405–414 (2006).
27. F. V. Ignatovich and L. Novotny, "Real-Time and Background-Free Detection of Nanoscale Particles," Phys. Rev. Lett. **96**, 013901 (2006).
28. H. Ewers, V. Jacobsen, E. Klotzsch, A. E. Smith, A. Helenius, and V. Sandoghdar, "Label-free Optical Detection and Tracking of Single Virions Bound to their Receptor in Supported Membrane Bilayers," Nano Lett. **7**, 2263–2266 (2007).
29. S. Schultz, D. R. Smith, J. J. Mock, and D. A. Schultz, "Single-target molecule detection with nonbleaching multicolor optical immunolabels," PNAS **97**, 996–1001 (2000).
30. C. Sönnichsen, S. Geier, N. E. Hecker, G. von Plessen, J. Feldmann, H. Ditlbacher, b. Lamprecht, J. R. Krenn, F. R. Aussenegg, V. Z.-H. Chan, J. P. Spatz, and M. Möller, "Spectroscopy of single metallic nanoparticles using total internal reflection microscopy," Appl. Phys. Lett. **77**, 2949–2951 (2000).

The progress of nanoscience and technology in the past two decades has been accompanied by a growing interest in the optical study of single nano-objects[1]. A major thrust in this research area came from cryogenic spectroscopy [2, 3] as well as room temperature detection [4] and microscopy[5, 6] of dye molecules. Although a fluorescent atom suspended in vacuum can be seen even by the naked eye, achieving a high signal-to-noise ratio (SNR) in the detection of single molecules is a nontrivial task in the condensed phase. In particular, the background light and noise associated with the fluorescence or scattering from the environment can easily dominate the small signal of a single emitter. Furthermore, the dark counts and noise of photodetectors put a limit on the lowest signals that one might hope to detect.

As shown in Fig. 1(a), the level scheme of a fluorescent molecule consists of vibrational manifolds in the electronic ground (g) and excited (e) states. For an appropriate combination of an emitter and its surrounding matrix, the linewidth of the so-called zero-phonon line (ZPL) of the 0-0 transition between the vibrational ground states of g and e can become lifetime limited at cryogenic temperatures, thus enhancing the emitter's absorption cross section σ [7]. A very successful method for detecting a single molecule with a narrow 0-0 ZPL has been fluorescence excitation spectroscopy [3] where the red-shifted incoherent fluorescence of the molecule at wavelength λ_{red} is separated from the light at the laser wavelength λ_{las} by using high quality spectral filters. The noise of this technique is limited by the detector dark counts, which can be as low as 20-100 counts per second (cps) for very good avalanche photodiode single photon counters. The signal can reach up to typical values of $10^5 - 10^6$ cps on the detector for a good dye molecule dictated by saturation. Thus, fluorescence excitation spectroscopy can enjoy a very healthy SNR when applied to strongly fluorescent systems. Detection of very weak emitters, however, remains a challenge. In particular, fluorescence detection of single rare earth ions has been hampered owing to their long lifetimes and therefore ultra weak fluorescence.

An alternative approach to the detection of single solid-state emitters is to go back to the first method that was applied in single molecule spectroscopy [2], namely to detect the extinction

#98684 - $15.00 USD Received 11 Jul 2008; revised 18 Sep 2008; accepted 27 Sep 2008; published 14 Oct 2008

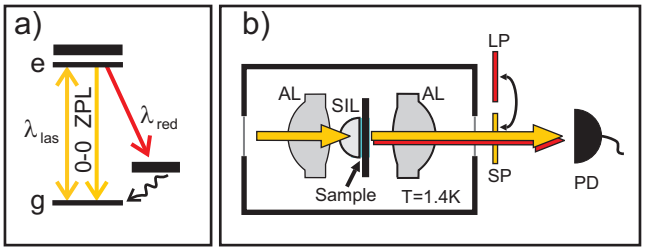

Fig. 1. (a) The level scheme of a dye molecule. (b) The schematics of our experimental setup. A laser beam is focused onto the sample using an aspheric lens (AL) and a hemispherical solid-immersion lens (SIL). A second aspherical lens is used to collect the transmitted laser beam as well as the forward emitted fluorescence of the molecule. LP: long pass filter, SP: short pass filter, PD: photodetector.

of the laser light caused by a single molecule in its path. This method was successfully revived by Plakhotnik and Palm in 2001 [8] where the coherent scattering of the excitation light was interfered with the residual reflections from the interfaces in the setup. Closely related efforts followed on quantum dots, especially with the aim of acquiring access to the linewidth of the main optical transition in these systems [9, 10]. Recently, we have extended this approach to detect the extinction of a laser beam by a single molecule in transmission without the need for any noise suppression technique [11, 12, 13]. In this paper, we compare the conventional fluorescence excitation technique with extinction measurements in terms of the SNR and discuss the potential of the latter for detecting emitters with very weak optical transitions.

The experimental arrangement of our discussion is depicted in Fig. 1(b), and its details are described in Refs. [11, 13]. Briefly, the excitation laser light was focused onto the sample consisting of DBATT molecules embedded in a *n*-tetradecane matrix inside a cryostat. For this we used an aspheric lens with a numerical aperture of 0.68 and a cubic zirconia hemispherical solid immersion lens (SIL). After interaction with the sample, a second aspheric lens collimates the beam and directs it to an avalanche photodiode (PD). Two different filter sets are used to either reject $\lambda_{\rm las} \sim 590$ nm and detect $\lambda_{\rm red} > 600$ nm or vice versa. The former arrangement delivers a fluorescence excitation spectrum while the latter allows a direct resonant measurement. Figure 2 shows examples of fluorescence and extinction spectra recorded from the same single molecule. All measurements were performed on the same detector at three different incident powers and for 1 s integration time per pixel. In this article we adopt the unit of counts per second (cps) for power. When the detected laser power reads 10^6 cps on PD (corresponding to an excitation regime well below saturation) both extinction (a) and fluorescence (b) yield comparable SNR. For a detected laser power of 3.2×10^4 cps, the fluorescence of the molecule is hardly above the detector dark count rate of 100 cps. However, the extinction is still easily observable at 10% visibility. Even at an ultra-low illumination level of 2000 cps the extinction signal succeeds in detecting the molecule whereas the fluorescence peak is fully buried under the detector noise.

Assuming a perfect transmission channel and detector, the power on PD in the absence of any spectral filter is given in cps by

$$\begin{aligned} P &= \frac{\varepsilon_0 c r^2}{2\hbar\omega} \int_\Omega \left(\left\langle \hat{\mathbf{E}}^-_{\rm las} \cdot \hat{\mathbf{E}}^+_{\rm las} \right\rangle + \left\langle \hat{\mathbf{E}}^-_{\rm m} \cdot \hat{\mathbf{E}}^+_{\rm m} \right\rangle + 2{\rm Re} \left\langle \hat{\mathbf{E}}^-_{\rm las} \cdot \hat{\mathbf{E}}^+_{\rm m} \right\rangle \right) d\Omega \\ &= P_{\rm las} + P^\Omega_{\rm m} - P_{\rm ext} \,, \end{aligned} \tag{1}$$

where $\hat{\mathbf{E}}^\pm_{\rm las}$ and $\hat{\mathbf{E}}^\pm_{\rm m}$ represent the positive and negative frequency components of the electric field operator associated with the laser and the molecular emission at the detector, respectively.

#98684 - $15.00 USD Received 11 Jul 2008; revised 18 Sep 2008; accepted 27 Sep 2008; published 14 Oct 2008

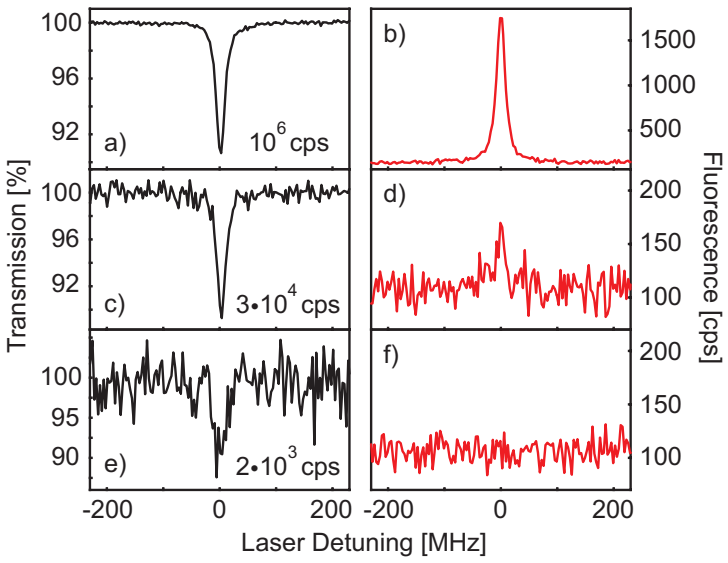

Fig. 2. a), c), e) Extinction spectra recorded from a single molecule in transmission at three different detected laser powers of 10^6, 3×10^4, 2×10^3 cps as measured on the detector. b), d), f) Fluorescence excitation spectra recorded under same conditions as spectra a), c), and e), respectively.

ω is the frequency of the emitted photon, and r is the radius of the reference sphere on which the solid angle integration is carried out. Ω denotes the solid angle of light collection and is assumed to cover all the transmitted laser light. The molecular emission $P_{\rm m}^{\Omega}$ consists of a part that originates from the 0-0 ZPL transition which is resonant with the laser light as well as a red-shifted component that results from molecular and lattice vibronic transitions. The electric field associated with the coherent part of the resonance fluorescence [13, 14] gives rise to a nonzero third term $P_{\rm ext}$ of Eq.(1), signifying the interference between the molecular emission and the laser beam. This component, which is known as the "extinction" term [15] is equivalent to a homodyne signal where the excitation laser beam acts as the local oscillator [16, 17].

It is helpful for the following discussion to write the terms of Eq. (1) in an explicit manner:

$$\begin{aligned}
P_{\rm las} &= \frac{\varepsilon_0 c r^2}{2\hbar\omega}\int_{\Omega}\left\langle \hat{\mathbf{E}}^{-}_{\rm las}\cdot\hat{\mathbf{E}}^{+}_{\rm las}\right\rangle d\Omega \\
P_{\rm m}^{4\pi} &= \frac{\varepsilon_0 c r^2}{2\hbar\omega}\int_{4\pi}\left\langle \hat{\mathbf{E}}^{-}_{\rm m}\cdot\hat{\mathbf{E}}^{+}_{\rm m}\right\rangle d\Omega = \Gamma_1\rho_{22} = \frac{\Gamma_1}{2}\frac{S}{1+S} \\
P_{\rm m}^{\Omega} &= \zeta P_{\rm m}^{4\pi} \\
P_{\rm m}^{\rm res} &= \alpha P_{\rm m}^{\Omega} \\
P_{\rm m}^{\rm red} &= (1-\alpha)P_{\rm m}^{\Omega} = \zeta(1-\alpha)\frac{\Gamma_1}{2}\frac{S}{1+S} \\
P_{\rm ext} &= -\frac{\varepsilon_0 c r^2}{2\hbar\omega}\int_{\Omega} 2{\rm Re}\left\langle \hat{\mathbf{E}}^{-}_{\rm las}\cdot\hat{\mathbf{E}}^{+}_{\rm m}\right\rangle d\Omega\,. \qquad (2)
\end{aligned}$$

The quantity $P_{\rm m}^{4\pi}$ gives the total power emitted by the molecule into the 4π solid angle. ρ_{22} is the population of the excited state, and the on-resonance saturation parameter S reads [14]

$$S = \frac{\mathscr{V}^2}{\Gamma_1\Gamma_2}, \qquad (3)$$

#98684 - $15.00 USD Received 11 Jul 2008; revised 18 Sep 2008; accepted 27 Sep 2008; published 14 Oct 2008

where $\mathscr{V}$ is the Rabi frequency defined by $\hbar\mathscr{V} = d_{\mathrm{ZPL}} \cdot E_{\mathrm{las}}(\mathrm{O})$. The transition dipole moment d_{ZPL} and the incident electric field $E_{\mathrm{las}}(\mathrm{O})$ at position of the molecule are assumed to be parallel for simplicity. The factor α describes the ratio of the power emitted on the 0-0 ZPL to the total excited state emission. Thus, $d_{\mathrm{ZPL}} = \sqrt{\alpha} d_{\mathrm{eg}}$ where d_{eg} denotes the dipole moment associated with the total spontaneous emission rate of the excited state given by $\Gamma_1 = d_{\mathrm{eg}}^2 \omega^3/(3\pi\varepsilon_0\hbar c^3)$. Γ_2 represents the transverse decay rate which equals $\Gamma_1/2$ in the absence of any dephasing. The parameter ζ signifies the fraction of the total emitted molecular power to that collected into the detection solid angle Ω. We note that in addition, one might have to account for total internal reflection and waveguiding in the substrate which influence the angular distribution of the laser light and the molecular emission [11]. Finally, the quantities $P_{\mathrm{m}}^{\mathrm{res}}$ and $P_{\mathrm{m}}^{\mathrm{red}}$ represent the portions of the molecular emission into the solid angle Ω that are resonant with the excitation laser and red shifted from it, respectively.

It is now instructive to separate the properties of the laser beam from the spectroscopic features of the emitter. Using the definitions of Γ_1 and $\mathscr{V}$, one can rearrange the saturation parameter in Eq. (3) to read

$$S = \frac{\alpha}{\Gamma_2} \mathscr{K} P_{\mathrm{las}} \,, \tag{4}$$

where $\mathscr{K}$ is a unitless geometrical factor that relates $|E_{\mathrm{las}}(\mathrm{O})|^2$ to the laser power P_{las}. More precisely, $\mathscr{K}$ denotes the ratio of the total power scattered by a weakly excited two-level system and the incident power. It depends on the spatial mode of the laser beam and the focusing optics. The reader is referred to Ref. [18] for details.

The expressions in Eq. (2) provide us with the red-shifted fluorescence power $P_{\mathrm{m}}^{\mathrm{red}}$ and its dependence on the experimental variables ζ and S and the molecular properties α and Γ_1. The corresponding noise N_{red} is composed of the shot noise of the fluorescence and of the fluctuations in the detector's dark counts P_{drk} if we assume that the excitation light is completely rejected by the filters. Thus, the SNR for a fluorescence excitation measurement becomes

$$\mathrm{SNR}_{\mathrm{red}} = \frac{\mu P_{\mathrm{m}}^{\mathrm{red}}}{N_{\mathrm{red}}} = \begin{cases} \dfrac{\mu\zeta(1-\alpha)\Gamma_1}{2\sqrt{P_{\mathrm{drk}}}} \dfrac{S}{1+S} \,, & \mu P_{\mathrm{red}} \ll P_{\mathrm{drk}} \\ \sqrt{\dfrac{\mu\zeta(1-\alpha)\Gamma_1}{2} \dfrac{S}{1+S}} \,, & \mu P_{\mathrm{red}} \gg P_{\mathrm{drk}} \,, \end{cases} \tag{5}$$

where we have introduced μ to account for losses (e.g. cryostat windows, filters, etc.) and the detector efficiency. The SNR increases typically first linearly with S when $P_{\mathrm{m}}^{\mathrm{red}} < P_{\mathrm{drk}}$, then with $\sqrt{S}$ and reaches a maximum in the fully saturated regime.

Assuming that the solid angle Ω collects all the incident laser light, a simple energy balance argument implies that P_{ext} in Eq. (1) must correspond to the total power $P_{\mathrm{m}}^{4\pi}$ emitted by the molecule. Now we insert a spectral filter to select only the part of the transmitted light that is resonant with the laser light. Denoting the size of the dip in the power that is detected in this case by $P_{\mathrm{dip}}^{\mathrm{res}}$, Eq. (1) and Eqs. (2) yield,

$$P_{\mathrm{dip}}^{\mathrm{res}} = P_{\mathrm{ext}} - P_{\mathrm{m}}^{\mathrm{res}} = P_{\mathrm{m}}^{4\pi} - P_{\mathrm{m}}^{\mathrm{res}} = (1-\alpha\zeta)\frac{\Gamma_1}{2}\frac{S}{1+S} \,. \tag{6}$$

The noise on a resonant extinction measurement is composed of the shot noise $\sqrt{\mu(P_{\mathrm{las}} - P_{\mathrm{dip}}^{\mathrm{res}})}$ of the detected signal, the fluctuations $\mu\kappa(P_{\mathrm{las}} - P_{\mathrm{dip}}^{\mathrm{res}})$ on the laser intensity with κ as a proportionality constant, and the fluctuations $\sqrt{P_{\mathrm{drk}}}$ of the detector dark counts. Since these contributions are statistically independent, the total noise can be written as

$$N_{\mathrm{res}} = \sqrt{\mu(P_{\mathrm{las}} - P_{\mathrm{dip}}^{\mathrm{res}}) + \mu^2\kappa^2(P_{\mathrm{las}} - P_{\mathrm{dip}}^{\mathrm{res}})^2 + P_{\mathrm{drk}}}, \tag{7}$$

#98684 - $15.00 USD Received 11 Jul 2008; revised 18 Sep 2008; accepted 27 Sep 2008; published 14 Oct 2008

where again, μ accounts for losses and the detection efficiency. Assuming that the laser intensity fluctuations have been mastered at a sufficient level and that $P_{\rm las} \gg P_{\rm dip}^{\rm res}$, one finds $N_{\rm res} \simeq \sqrt{\mu P_{\rm las}}$. Thus, the signal-to-noise ratio for an extinction measurement becomes

$$\mathrm{SNR}_{\rm res} = \frac{\mu P_{\rm dip}^{\rm res}}{N_{\rm res}} \simeq (1-\zeta\alpha)\frac{\Gamma_1}{2}\sqrt{\frac{\mu\alpha\mathscr{K}}{\Gamma_2}}\frac{\sqrt{S}}{1+S}\,. \tag{8}$$

The circles in Fig. 3(a) present $\mathrm{SNR}_{\rm res}$ as a function of the detected laser power $\mu P_{\rm las}$ and of the saturation parameter S. In each case, S was directly derived from the power broadened linewidth of the fluorescence excitation spectrum. The data were recorded by adding 100 scans with 10 ms integration time, corresponding to a total acquisition time of 1 second per frequency pixel. This procedure helped to correct for possible laser drifts and spectral diffusion of the molecule. The nonlinearity of the APD was rigorously compensated by comparing the response of a separate linear photodiode from a split beam of much higher power. For the data points higher than 10^6 cps, we added neutral density filters after the cryostat. We fitted each spectrum with a Lorentzian function and used its peak value as the signal size. The square root of the signal was assigned to the noise since our system could perform at the shot-noise limit down to the sub Hertz bandwidth over the whole power range presented here.

The green theoretical fit curve is obtained using Eq. (8). With the parameters that have been independently determined for our setup ($\mu = 0.2$, $\mathscr{K}$=0.5, $\alpha = 0.2$, $\zeta = 0.02$, $\Gamma_2 = \Gamma_1/2, \Gamma_1/2\pi = 17$ MHz), an excellent agreement with the measured data is achieved. The behavior of $\mathrm{SNR}_{\rm res}$ under very strong excitation crossing over from a $S^{1/2}$ to a $S^{-1/2}$ dependence is clearly visible. This crossover stems from the fact that for a quantum emitter, $P_{\rm dip}^{\rm res}$ saturates at high incident powers. The maximal attainable SNR in a shot-noise limited resonant detection then becomes $\mathrm{SNR}_{\rm res}^{\rm max} = \sqrt{\Gamma_1^2\alpha\mathscr{K}\mu/(16\Gamma_2)}$ and occurs at S=1 if we assume $\zeta\alpha \ll 1$.

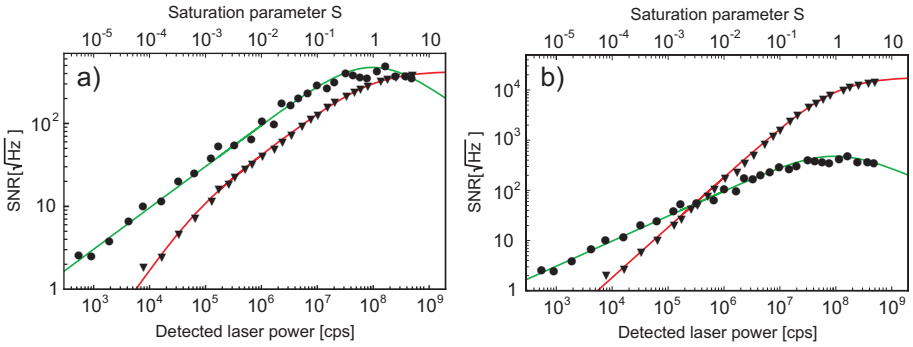

Fig. 3. The signal-to-noise ratios of the resonant transmission (circles, green lines) and fluorescence (triangles, red lines) signals as a function of the excitation power and saturation parameter for two different definitions of noise: (a) noise determined from the fluctuations of the signal on resonance, (b) noise evaluated from the fluctuations of the off-resonant background. Symbols display the experimental data and the lines denote the theoretical behavior.

To compare the SNR of fluorescence and extinction measurements directly, in Fig. 3(a) we also present by triangles the $\mathrm{SNR}_{\rm red}$ obtained from fluorescence spectra recorded at the same excitation powers as their extinction counterparts. The signal and the noise were determined according to the same procedure mentioned above for the extinction measurements. The fitted red curve follows from Eqs. (5) and gives a very good agreement with the experimental data over many orders of magnitude. It is evident that in the weak excitation regime where detector

#98684 - $15.00 USD Received 11 Jul 2008; revised 18 Sep 2008; accepted 27 Sep 2008; published 14 Oct 2008

dark count becomes considerable, the homodyne advantage of extinction measurements leads to a superior SNR as compared to fluorescence detection. However, we also find that the SNR of extinction measurements wins in the case of stronger excitations up to saturation. This might seem unexpected in view of the fact that two decades of solid-state single emitter spectroscopy has nearly exclusively relied on fluorescence measurements. Here, one has to keep in mind that contrary to the conventional experiments, we have achieved a substantial $\mathscr{K}$ by strong focusing [13]. In general, the competition between the performances of fluorescence and extinction measurements is decided by many factors entering equations 5 and 8. At this point, we find it interesting to point out that the exact definition of SNR can also affect the outcome of such a comparison. In the existing literature, the rms fluctuation of the signal has been often included as a noise source in fluorescence but ignored in extinction measurements [19, 20]. In our comparison of the two methods presented in Fig. 3(a), we have consistently chosen to define the signal as the response of the emitter and the noise as its fluctuations at the resonant frequency, originating from all sources. A reasonable alternative measure for the detectability of a single emitter could also be to compare the signal only to the noise associated with the off-resonant background, i.e. neglecting the fluctuations of the signal. In Fig. 3(b) we have analyzed the same experimental data according to this latter strategy and have fitted them using a correspondingly modified version of equations 5 and 8. In this intuitive measure, fluorescence detection seems advantageous at higher power. Finally, we point out in passing that both $\mathrm{SNR}_{\mathrm{red}}$ and $\mathrm{SNR}_{\mathrm{res}}$ scale as the square root of the integration time and thus, the comparison between the fluorescence and extinction methods holds for fast and slow measurements alike.

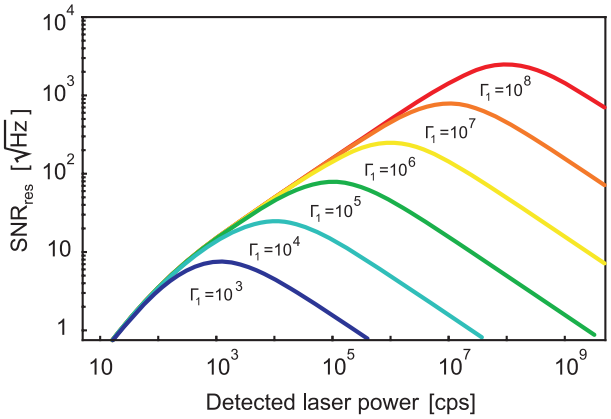

Fig. 4. The SNR for a resonant transmission detection of emitters with different radiative decay rates. Here we have assumed $\alpha = \mu = 1$, P_{drk}=20 cps, and $\mathscr{K} = 0.5$. Γ_1 is given in units of rad/sec.

An exciting question that arises is whether extinction detection opens doors for studying weakly fluorescent nano-objects. Conventional single molecule detection has been successful for molecules that have fluorescence lifetimes of a few nanoseconds, corresponding to $\Gamma_1/2\pi \sim 10-100$ MHz. Such a high photon flux provides a good SNR even considering realistic collection plus detection efficiency of a few percent and $P_{\mathrm{drk}} = 100$ cps. However, for weakly emitting systems such as rare earth ions with lifetimes of the order of milliseconds, $\mathrm{SNR}_{\mathrm{red}}$ becomes comparable or smaller than unity. Figure 4 displays the expected $\mathrm{SNR}_{\mathrm{res}}$ as a function of the detected laser power for various radiative decay rates Γ_1. Here we have assumed a laboratory value of $\mathscr{K} = 0.5$, $\alpha = \mu = 1$, $\Gamma_2 = \Gamma_1/2$, and $P_{\mathrm{drk}} = 20$ cps, but extension of the results to other situations is straightforward by following Eq. (8). These plots indicate that single emitters

#98684 - $15.00 USD Received 11 Jul 2008; revised 18 Sep 2008; accepted 27 Sep 2008; published 14 Oct 2008

with spontaneous emission times as long as a millisecond should be detectable using extinction spectroscopy even when realistic detection parameters (e.g. $\mathscr{K} = 0.5, \alpha = 0.5, \mu = 0.2$) are considered. In addition, we emphasize that extinction measurements have the great added value that they provide direct access to the coherent interaction of the incident light and the emitter.

Although the basic concepts discussed in this paper have been known in signal processing and electrical engineering [16], their direct experimental investigations at the single emitter level have been made possible through advances in cryogenic spectroscopy [8, 13, 21]. Inspired by this progress, very recently we have also succeeded in extinction detection of a single solid-state quantum emitter at room temperature [22] despite the fact that the extinction cross section is reduced by 5-6 orders of magnitude due to severe broadening of the transition ($\Gamma_2 \gg \Gamma_1$). Another interesting application of extinction or homodyne detection has been demonstrated independently for imaging small metallic and dielectric nanoparticles [23, 24, 25, 26, 27, 28]. Conventional methods of nanoparticle detection such as dark-field [29] or total internal reflection [30] microscopy rely on the elimination of the incident light from the detection path and the detection of the power scattered by the particles. To this end, these techniques are analogous to fluorescence excitation spectroscopy where frequency spectra are replaced by spatial images, and spatial filtering substitutes spectral filtering for the discrimination of the incident laser light. However, in practice the two systems are limited in different ways because in the case of spatial imaging, the persistent source of ”noise” is the light scattered from residual optical roughness of the medium [26]. The equivalent of this problem usually does not arise in extinction detection of emitters because they are typically embedded in well-behaved matrices [1, 2] without any optical transitions in the spectral region of interest.

In conclusion, we have explored the signal-to-noise ratio in the spectroscopic detection of single emitters. We have provided expressions for evaluating the performance of both fluorescence and extinction measurements. In particular, we have demonstrated that extinction measurements can be superior to fluorescence detection in the weak excitation regime. Furthermore, we have shown that even weakly fluorescent emitters should be detectable using coherent extinction spectroscopy. This prospect is especially interesting for the optical storage and read out of quantum information in new systems such as rare earth ions.

This work was supported by the Swiss National Foundation (SNF).

#98684 - $15.00 USD Received 11 Jul 2008; revised 18 Sep 2008; accepted 27 Sep 2008; published 14 Oct 2008